

SYNOPSIS

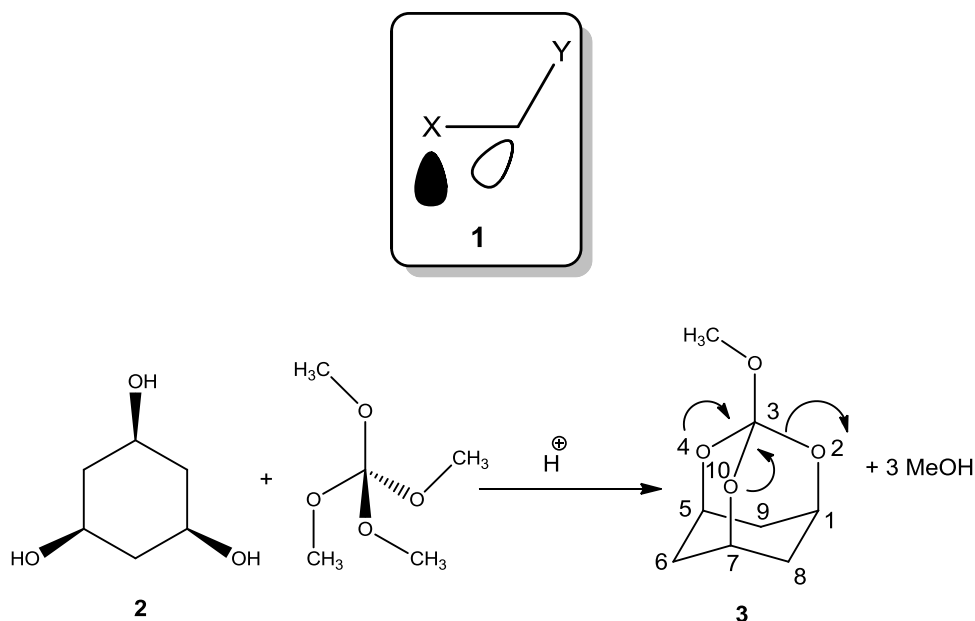
The thesis entitled ‘Crystal Structures as Mechanistic Probes: Anomeric effects, Antiaromaticity, Molecular Inclusion and Other Studies’ consists of four chapters. They describe various physical-organic studies which employ X-ray diffraction (XRD) as a key technique to arrive at mechanistic conclusions. The contents of each chapter are briefly discussed below.

Chapter 1. The anomeric effect in two rigid tricyclic systems: a trioxaadamantane and hexamethylenetetramine.

Although the anomeric effect was first demonstrated in the sugars, it is now recognized as a general phenomenon of fundamental importance that determines both ground state properties and reactivity. The anomeric interaction is firmly rooted in the antiperiplanar lone pair hypothesis (ALPH), which proposes an overlap between a lone pair of electrons and a vicinal σ^* orbital. (This would be the LUMO of a carbon-heteroatom bond, *cf.* **1**, Scheme 1).¹ In acyclic systems, the anomeric effect is often stymied by competing conformational changes, but is manifested in rigid analogues. Two interesting rigid tricyclic systems, in which conformational freedom is largely or completely eliminated, have been studied herein as described below.

Part A:

3-Methoxy-2,4,10-trioxaadamantane (**3**) is a stable tricyclic orthocarbonate that can be prepared from the corresponding cyclohexanetriol (**2**) and tetramethyl orthocarbonate [C(OMe)₄] as shown.² (Compounds such as **3** are stable analogues of the tetrahedral intermediates that are believed to be generally formed in acyl-exchange reactions, *e.g.* ester hydrolysis). In **3** a number of anomeric interactions are possible in principle (as indicated by the curly arrows), although one of them can be ruled out on geometrical grounds. Thus, the oxygen atoms of the trioxaadamantane unit can function as both donors and acceptors among themselves. However, the exocyclic oxygen atom of the methoxy group can only function as a donor, as the σ^* orbital corresponding to the C-OMe bond is trapped inside the adamantyl cage: thus, the C-OMe bond is not antiperiplanar to any of the neighbouring lone pairs (being rather *gauche* to them).



Scheme 1. The anomeric effect as an overlap between a lone pair of electrons (shaded orbital in **1**, X and Y being heteroatoms) with an adjacent LUMO (unshaded orbital in **1**, σ^* of the C-Y bond). The formation of the trioxaadamantane **3** is also shown; from the triol **2** and methyl orthocarbonate [C(OMe)₄]; the curly arrows in **3** represent electron flow via the anomeric effect

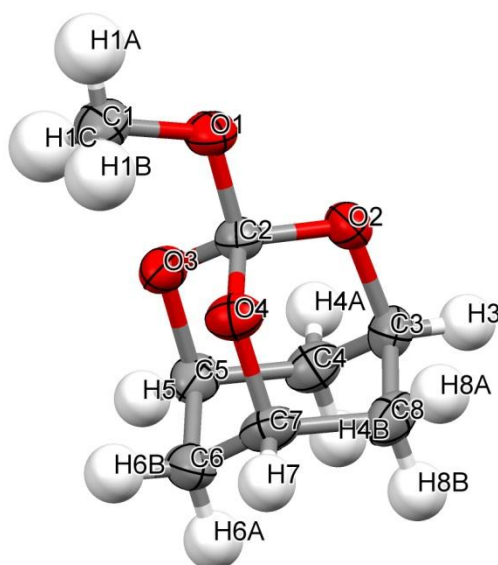


Fig. 1. ORTEP diagram of the methoxyadamantane **3**, as determined by single crystal XRD

In the crystal structure of **3** (Fig. 1),³ it was observed that all the four C-O bonds at the orthocarbonate centre (C_3) are shorter than the standard C-O bond length (1.43 Å). However the three endocyclic C-O bonds at C_3 are not uniformly short, O_2-C_3 (1.39 Å)

being shorter than O_4-C_3 and $O_{10}-C_3$ (both ~ 1.40 Å). The exocyclic $O-C_3$ bond, however, is the shortest at 1.37 Å, although the O -Me bond is normal at 1.43 Å.

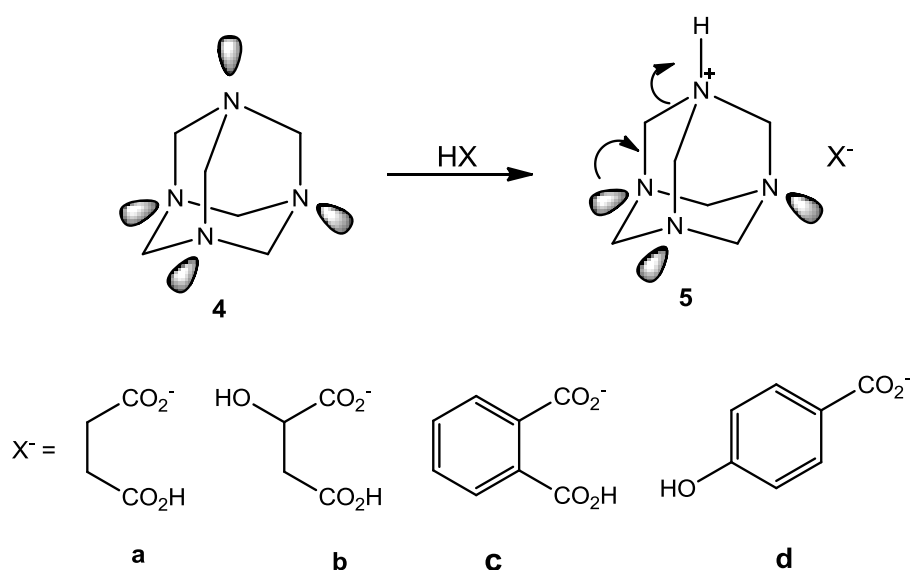
Intriguingly, the remaining three endocyclic C-O bonds (O_2-C_1 , O_4-C_5 and $O_{10}-C_7$) are unusually long at ~ 1.46 Å. These bonds, in fact, are essentially antiperiplanar to the exocyclic $O-C_2$ bond, i.e. parallel and in close proximity to the corresponding antibonding σ^* orbital that is ensconced within the adamantyl cage. The torsion angle for $C_{Me}-O-C_3-O_2$ (-176.4°) indicates that the OMe group is poised above and nearly midway between O_4 and O_{10} . This also indicates that the two lone pairs on the exocyclic oxygen atom are antiperiplanar to O_4-C_3 and $O_{10}-C_3$, the two longer of the three endocyclic C-O bonds (*vide supra*).

These results indicate that the predominant anomeric interaction in **3** involves the exocyclic oxygen atom as donor. The anomeric interaction involving the endocyclic oxygen atoms are less pronounced and, interestingly, asymmetrical.

Part B:

This part deals with ALPH as applied to hexamethylenetetramine (HMT, **4**, Scheme 2, also ‘urotropine’).⁴ In HMT each lone pair is antiperiplanar to 3 adjacent C-N σ^* orbitals (although each σ^* may overlap with only one lone pair). The rigidity and high symmetry in **4** indicate that the nitrogen centres act as both donors and acceptors. In particular, it was of interest to enquire how the system would respond to an electronic perturbation. This led to the preparation and crystallographic study of four salts of **4**, with succinic, DL-malic, phthalic and 4-hydroxybenzoic acids (**5a**, **5b**, **5c** and **5d** respectively, typified by Fig. 2).³

Interestingly, in all the above four structures, an elongation of the C-N bonds (~ 1.51 Å) around the protonated N centre, relative to the C-N bonds (~ 1.45 Å) attached to the corresponding donor N centres, was observed. This evidences the anomeric interaction indicated in **5**. Also, the selective elongation (~ 1.47 Å) of a C-N bond in which the N centre was involved in intermolecular H-bonding or a short contact, relative to a normal C-N bond (~ 1.44 Å), was observed. This apparently indicates a diminution of the donor ability of the protonated N centre.



Scheme 2. Hexamethylenetetramine **4** and its salts **5** with succinic (**a**), DL-malic (**b**), phthalic (**c**) and 4-hydroxybenzoic (**d**) acids; the shaded orbitals indicate the stereoelectronic orientation of the lone pairs of electrons on the various nitrogen centres; the curly arrows in **5** indicate electron flow by the anomeric interaction

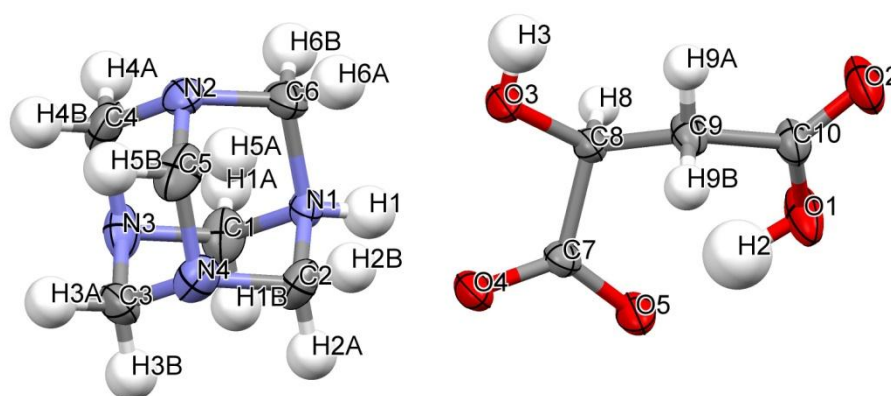
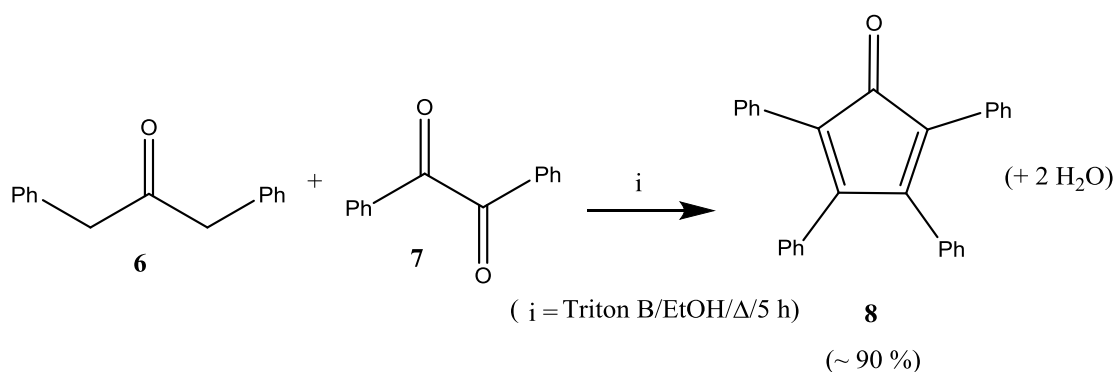


Fig. 2. ORTEP diagram of the urotropine-malic acid salt **5b** (by single-crystal XRD)

Chapter 2. Anti-aromaticity in tetraarylcyclopentadienones by single crystal X-ray diffraction and charge density analysis.

Tetraphenylcyclopentadienone (tetracyclone, **8**, Scheme 3) is a remarkable compound that is formed relatively easily and in high yields, despite its possessing the antiaromatic cyclopentadienone as its core moiety.⁵

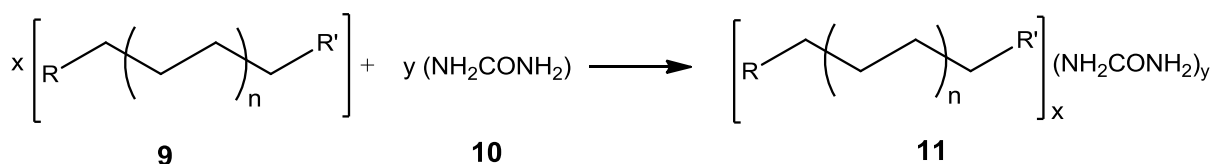


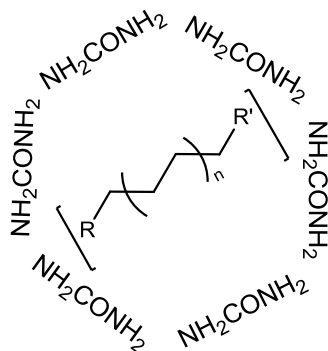
Scheme 3. The base-catalysed condensation of diphenylacetone (**6**) and benzil (**7**) to form tetracyclone (**8**)

It was thus of interest to determine the essential reason for the apparently stable existence and ease of formation of **8**. In particular, it was unclear whether the molecule possessed largely kinetic stability – deriving from the relatively large phenyl groups – or rather thermodynamic stability of unknown origin. In fact, it was possible that the formation of **8** was driven by its crystallisation, which indicated the possibility that the crystal lattice possessed a stability that overruled the molecular level anti-aromaticity of the core moiety. The details of the crystal packing were thus sought via X-ray diffraction.

In addition, several new descriptors (Quantum Theory of Atoms in Molecules, Nucleus Independent Chemical Shift, and Source Function) were applied to elucidate the anti-aromatic character of tetracyclone. All these indicated that, although the central cyclopentadienone core is anti-aromatic, the molecular level anti-aromaticity is possibly subdued by various non-covalent interactions within the crystal lattice.⁶

Chapter 3. New light on urea inclusion complexes: formation in the solid state and characterisation by IR, DSC and PXRD.





12

Scheme 4. The formation of a urea inclusion complex (**11**) via crystallisation of the guest (**9**) and urea host (**10**); **12** is a cartoon representation of **11**, indicating the hexagonal hydrogen-bonded channel formed by **10**, with the included **9**

The channel compounds formed between urea and many linear, unbranched host molecules represent a remarkable example of molecular inclusion that is both theoretically and practically intriguing (Scheme 4).⁷ The normally tetragonal crystal habit of urea (P4₂m) changes to hexagonal (P6₁22/P6₅22) upon the inclusion of the guest molecule, which is apparently stabilised by van der Waals forces between the immobilized guest and the inside of the host channel. The phenomenon has also found use in separating certain isomeric mixtures (*e.g.* mixture of fatty acids, 1- and 2-bromooctane) that are otherwise difficult to resolve.

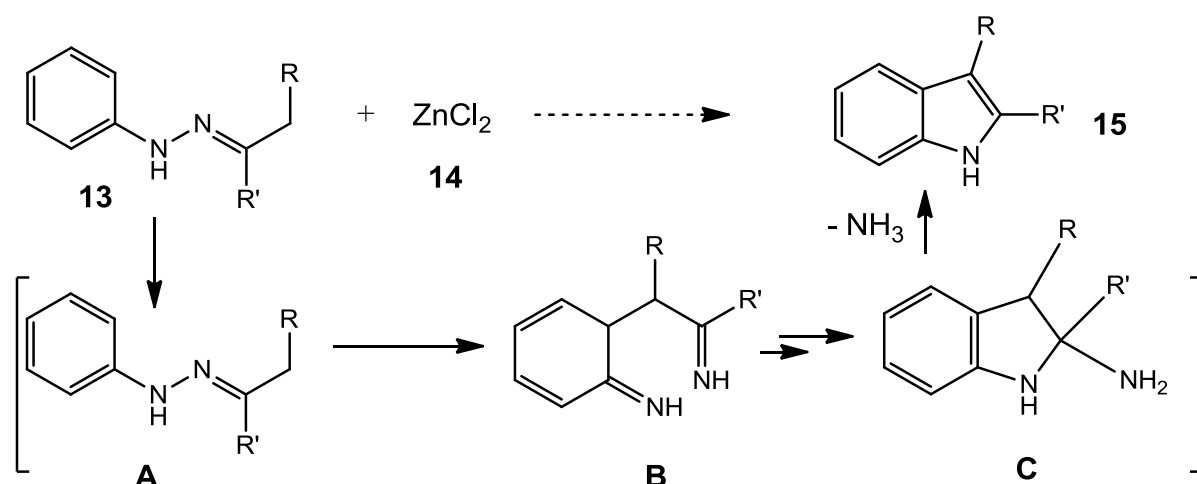
Generally, the urea complexes (**11**) have been prepared via co-crystallization from the solution state. In the present work, it is demonstrated that they can be formed by direct admixture of the host and guest components (in a particular ratio) in the solid state. This technique represents a considerable practical improvement, as the solution phase method is not only time-consuming but also suffers from solubility limitations. (Urea, being highly polar, needs a solvent such as MeOH, from which the usually non-polar host is not complexed and crystallized efficiently).

A liquid assisted grinding technique was also employed to effect the complexation. The small amount of solvent (in which urea is fairly soluble) employed in this technique apparently assists the diffusion of the guest molecules into the lattice of the host molecule. Theoretically, also, the success of the solid state technique is intriguing, as it demonstrates that the tetragonal-to-hexagonal lattice transformation can occur by a molecular reorganization via the diffusion of the guest molecules within it.

Infra-red (IR) spectra confirmed the formation of the complexes, via discernible shifts in the N-H and C=O bands. The ‘Differential Scanning Calorimetry (DSC)’ thermograms of the ground mixtures of urea and the long chain guest compounds showed a shift in the endotherm peak positions with respect to the components. In addition, certain changes in the ‘Powder X-ray Diffraction (PXRD)’ pattern were also observed. These evidence the formation of the complexes by the solid-state technique.

Chapter 4. Solid acid-catalysed improved one-pot Fischer indole synthesis.

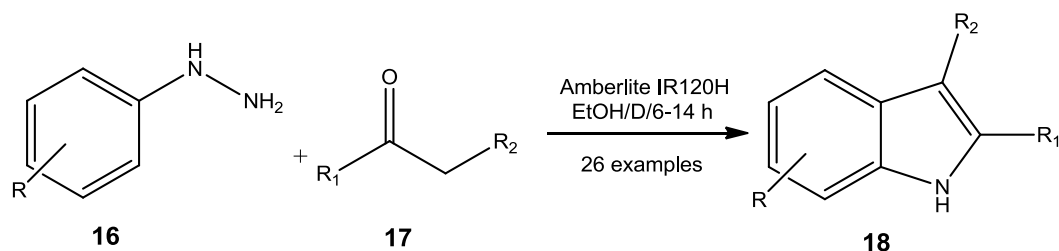
The classical Fischer indole synthesis is effected by heating a phenylhydrazone (**13**, Scheme 5) with an acid (typically **14**) in an appropriate solvent. The reaction occurs via a rearrangement-cleavage sequence, the key step being a [3,3]-sigmatropic rearrangement of **A** to **B**, which then cyclises to form the indole skeleton in **C**. Elimination of NH₃ finally leads to **15**.⁸



Scheme 5. The key steps in the Fischer indole synthesis, showing the Lewis acid (**14**) catalysed conversion of the phenylhydrazone **13** to the indole **15**

Considering the continued importance of various indole derivatives in chemistry and biology, it is always of interest to develop improved versions of the original method. In view of the simplicity of the overall transformation, a solid-state version of the transformation seemed feasible and worth exploring. The known solvent-free versions of the one-pot Fischer synthesis, however, usually require an excess of a protic/Lewis acid catalyst.⁹ A solid acid-catalysed one-pot Fischer indolisation, starting from enolizable ketones and phenylhydrazines apparently offered promise.

A few strongly acidic cation exchange resins were thus tested. Finally, after optimising the reaction conditions, Amberlite® IR120 was chosen as the solid acid catalyst in refluxing ethanol. This strategy was applied to synthesise a number of indoles starting from various aliphatic, alicyclic and aromatic ketones, as also a few aliphatic aldehydes (Scheme 6), results being summarised in Table 1.

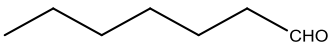
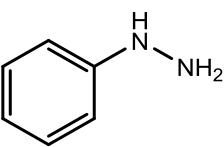
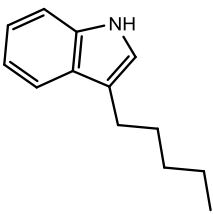
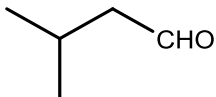
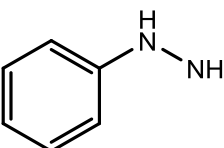
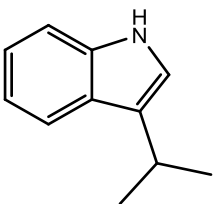
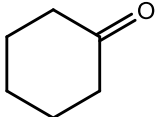
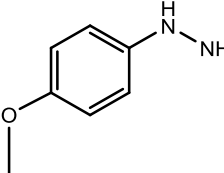
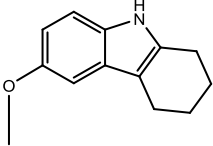
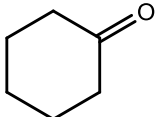
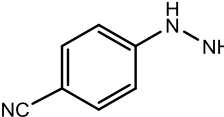
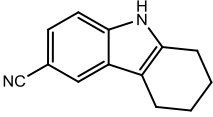
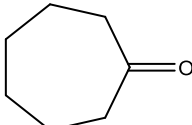
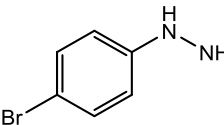
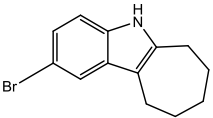
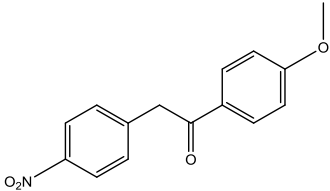
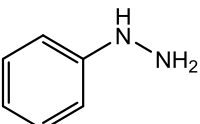
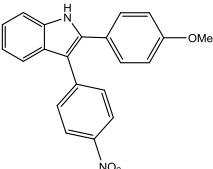
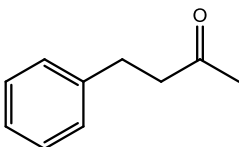
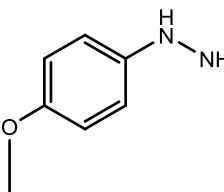
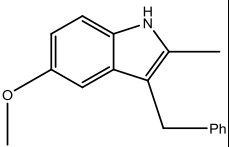


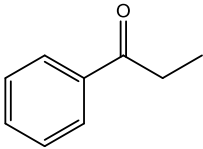
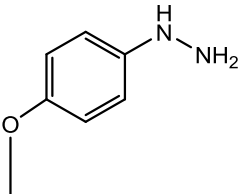
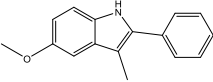
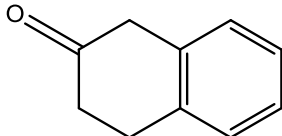
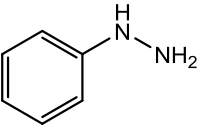
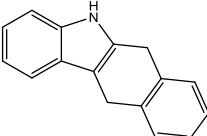
Scheme 6. The one-pot Fischer indole synthesis with Amberlite resin

Table 1. Fischer indole synthesis: conditions and yields

Entry	Ketone	Phenylhydrazine	Product	Time (h)	Yield (%)
1				8	82
2				10	75

Table 1 (Contd.)

3				6	72
4				6	70
5				10	85
6				14	80
7				10	88
8				14	72
9				7	85

10				6	88
11				10	86

REFERENCES

1. Chandrasekhar, S. *Arkivoc* **2005**, *xiii*, 37-66.
2. Chandrasekhar, S.; Roy, C. D. *Indian J. Chem. B* **1995**, *34 B*, 171-172.
3. Details of the crystallographic studies reported herein may be obtained from the Cambridge Crystallographic Data Centre (e-mail: deposit@ccdc.cam.ac.uk), by quoting the nos. 1001293 (**3**), 1011279 (**5a**), 1002361 (**5b**), 1009743 (**5c**) and 1012196 (**5d**).
4. Terpstra, M.; Craven, B. M.; Stewart, R. F. *Acta Cryst.* **1993**, *A49*, 685-692.
5. Smith, M. B.; March, J. *March's Advanced Organic Chemistry: Reactions, Mechanisms and Structure*, 6th ed.; John Wiley: Hoboken, 2007; pp 54-95.
6. Pal, R.; Mukherjee, S.; Chandrasekhar, S.; Guru Row, T. N. G. *J. Phys. Chem. A* **2014**, *118* (19), 3479-3489.
7. (a) Ref. 5, pp 126-127. (b) Hollingsworth, M. D.; Harris, K. D. M. In *Comprehensive Supramolecular Chemistry*; Atwood, J. L.; Bishop, R.; Davies, J. E. D.; Lehn, J.-M.; MacNicol, D. D.; Toda, F.; Vögtle, F., Eds.; Pergamon: Oxford, 1996; Vol. 6, pp 177-237.
8. (a) Ref. 5, pp 1674-1676. (b) Sundberg, R. J. In *Comprehensive Heterocyclic Chemistry*; Katritzky, A. R.; Rees, C. W.; Bird, C. W.; Cheeseman, G. W. H., Eds. Pergamon: Oxford, 1984; Vol. 4, pp 334-338.
9. Matsumoto, K.; Tanaka, A.; Yukio, I.; Hayashi, N.; Toda, M.; Bulman Robert, A. *Heterocycl. Commun.* **2003**, *9*, 9-12.